

# 1      The biosynthetic gene cluster of the C-nucleoside antibiotic

## 2      pyrazomycin with a rare pyrazole moiety

3

4      Guiyun Zhao<sup>[a],[e]</sup>, Shunyu Yao<sup>[a],[e]</sup>, Kristina W Rothchild<sup>[b]</sup>, Tengfei Liu<sup>[c]</sup>, Yu Liu<sup>[d]</sup>, Jiazhang  
5      Lian<sup>[c]</sup>, Hai-Yan He<sup>[b]</sup>, Katherine S Ryan<sup>[b]</sup>, Yi-Ling Du<sup>[a]\*</sup>

6

7      <sup>[a]</sup>Institute of Pharmaceutical Biotechnology and The First Affiliated Hospital, Zhejiang University School of  
8      Medicine, Hangzhou, China.

9      <sup>[b]</sup>Department of Chemistry, The University of British Columbia, Vancouver, British Columbia, Canada.

10     <sup>[c]</sup>Institute of Biological Engineering, College of Chemical and Biological Engineering, Zhejiang University,  
11     Hangzhou, China.

12     <sup>[d]</sup>College of Life Sciences, Zhejiang University, Hangzhou, China.

13     <sup>[e]</sup>These authors contributed equally to this work

14     \*Corresponding Author: yldu@zju.edu.cn

15

### 16     ● Abstract

17     Pyrazomycin is a rare C-nucleoside antibiotic with a naturally occurring pyrazole ring, whose  
18     biosynthetic origin has remained obscure for decades. In this study, we report the identification of  
19     the gene cluster responsible for pyrazomycin biosynthesis in *Streptomyces candidus* NRRL 3601,  
20     revealing that StrR-family regulator PyrR is the cluster-situated transcriptional activator governing  
21     pyrazomycin biosynthesis. Furthermore, our results from *in vivo* reconstitution and stable-isotope  
22     feeding experiments support that PyrN is a new nitrogen-nitrogen bond forming enzyme linking the  
23     ε-NH<sub>2</sub> nitrogen of L-*N*<sup>6</sup>-OH-lysine and α-NH<sub>2</sub> nitrogen of L-glutamate. This study lays the  
24     foundation for further genetic and biochemical characterization of pyrazomycin pathway enzymes  
25     constructing the characteristic pyrazole ring.

26

### 27     ● Main text

28     Nitrogen-nitrogen (N-N) containing natural products are group of specialized metabolites with  
29     diverse structures and a variety of biological activities.<sup>[1]</sup> These molecules have been isolated from

30 different sources, including bacteria, fungi and plants. Despite extensive studies on the genetic and  
31 biochemical basis of natural product biosynthesis over the past three decades, the biochemical routes  
32 leading to enzymatic N-N bond formation are only starting to be revealed.<sup>[2-14]</sup> We recently reported  
33 a heme-dependent piperazate synthase responsible for N-N cyclization in piperazic acid, a building  
34 block for many nonribosomal peptide (NRP) or NRP-polyketide hybrid molecules (**Fig. 1**).<sup>[2]</sup> The  
35 biosynthetic route to piperazate begins with the *N*-hydroxylation of L-ornithine, giving a  
36 hydroxylamine precursor, which is reminiscent of valanimycin biosynthesis, which also begins with  
37 a hydroxylamine precursor.<sup>[9]</sup> By contrast, N-N bond formation in other N-N bond containing  
38 natural products including compounds cremeomycin, fosfazinomycin and kinamycin starts instead  
39 with the generation of nitrous acid,<sup>[5,6,8,10]</sup> and the biosynthesis of the *N*-nitroso streptozocin  
40 originates with oxidation of the guanidine of L-arginine.<sup>[3,4]</sup> However, whether other pathways to N-  
41 N bond containing molecules might begin from hydroxylamine precursors was unknown. Recent  
42 studies into hydrazone unit formation in the dipeptide s56-p1 resulted in the discovery of a pathway  
43 that links the hydroxylamine L-*N*<sup>6</sup>-OH-Lys to hydrazino acetic acid formation.<sup>[7]</sup> In this pathway,  
44 Spb40, a fusion protein with cupin and aminoacyl-tRNA synthetase (aaRS)-like domains, appears  
45 from expression studies in *E. coli* to couple glycine and L-*N*<sup>6</sup>-OH-Lys by forming a N-N bond  
46 between the  $\alpha$ -NH<sub>2</sub> of glycine and the  $\epsilon$ -N atom of L-*N*<sup>6</sup>-OH-Lys, the latter of which is in turn  
47 generated by Spb38-catalyzed *N*<sup>6</sup>-hydroxylation of L-Lys. An Spb40-like enzyme was also reported  
48 in the gene cluster for triacsins, but the details of this reaction, and whether this type of enzymology  
49 might play a role in pathways to other N-N bond containing structures, remains obscure.<sup>[14]</sup>

50 Despite progress toward understanding the enzymology of N-N bond formation, biosynthetic  
51 routes to aromatic structures containing N-N bonds is largely unexplored. Construction of an N-N  
52 bond embedded in an aromatic ring might require a very different biosynthetic logic from formation  
53 of a hydrazine or other N-N linkage. Among N-N bond-containing structures, a key example is  
54 pyrazomycin (PZN, also known as pyrazofurin), a C-nucleoside with a rare pyrazole moiety.<sup>[15]</sup> As  
55 a nucleoside analog, PZN is a potent inhibitor of orotidine 5'-monophosphate decarboxylase and  
56 possesses broad-spectrum antiviral and antitumor activities.<sup>[16]</sup> Early biosynthetic studies on PZN  
57 and its structural analog formycin used isotope-labeled precursors to establish that the C-3 to C-6  
58 of the pyrazole ring in PZN derive from C-4 to C-1 of glutamate or  $\alpha$ -ketoglutarate. Similarly, the  
59 C-9, C-4, C-5, C-6 of the pyrazolopyrimidine ring in formycin derive from these precursors (**Fig.**

60 1).<sup>[17]</sup> However, the direct precursors of the two pyrazole nitrogen atoms and the biosynthetic  
61 machinery driving N-N bond formation have remained obscure.

62 To answer these long-standing questions, we sequenced the genome of the PZN producing  
63 strain *Streptomyces candidus* NRRL 3601, and identified a ~28 kb gene cluster as a candidate for  
64 the PZN biosynthetic gene cluster, which we name here as the *pyr* cluster (**Fig. 2a**, **Table S1**). This  
65 gene cluster carries a four-gene sub-cluster (*pyrOPQS*) that has been linked to the biosynthesis of  
66 coformycin, whose production seems to be associated with many nucleoside family natural  
67 products.<sup>[17-19]</sup> Moreover, the *pyr* cluster also contains *pyrE*, which shows sequence homology to  
68 genes encoding β-ribofuranosylaminobenzene 5'-phosphate (β-RFAP) synthase. In the biosynthesis  
69 of methanopterin, β-RFAP synthase catalyzes the condensation of *p*-aminobenzoic acid with  
70 phosphoribosylpyrophosphate through a *C*-glycosidic linkage.<sup>[20]</sup> A similar reaction for *C*-  
71 glycosidic bond formation seems to be also required during PZN biosynthesis. Furthermore, another  
72 interesting feature about the *pyr* cluster is the presence of *spb38* and *spb40* homolog genes *pyrM*  
73 and *pyrN*, indicating that this cluster encodes a potential hydrazine-producing pathway analogous  
74 to that of the s56-p1 pathway, which is also consistent with the N-N bond containing structure of  
75 PZN.<sup>[7]</sup> We note that the *pyr* cluster share many homologous genes with the recently reported  
76 formycin biosynthetic gene cluster (*for* cluster).<sup>[19]</sup> Considering the great structural similarity  
77 between pyrazomycin and formycin, it is not unexpected that they utilize similar biosynthetic genes.  
78 Taken together, our *in silico* analysis suggests that the *pyr* cluster might be responsible for PZN  
79 assembly in *S. candidus* NRRL 3601.

80 Although strain *S. candidus* NRRL 3601 was known as a PZN producer, we failed to detect  
81 any PZN production with various media we tested, including the one used in early studies (**Fig. 2b-**  
82 **2d**).<sup>[15]</sup> Introduction of a vector carrying the whole putative *pyr* cluster into the common  
83 *Streptomyces* host *S. albus* J1074 also did not produce any detectable PZN. To explore why no PZN  
84 is produced, we isolated total RNA from *S. candidus* NRRL 3601 and performed transcriptional  
85 analysis of the *pyr* cluster by RT-PCR. We found that most of the *pyr* genes were not actively  
86 transcribed under the culture condition we used (**Fig. 2d**). We thus turned to regulatory engineering  
87 of the PZN pathway. Analysis of the *pyr* genes revealed the presence of a single putative  
88 transcriptional regulator *pyrR*, which shows sequence homology to StrR-family regulators. As the  
89 prototype of this family, the streptomycin biosynthesis regulator StrR is the transcriptional activator

90 controlling the expression of streptomycin biosynthetic genes by interacting with multiple promoter  
91 regions within the gene cluster.<sup>[21,22]</sup> Members of this family also include NovG and Bbr, which are  
92 located in the biosynthetic gene clusters of novobiocin and balhimycin, respectively.<sup>[23,24]</sup> This  
93 bioinformatic analysis suggested that *pyrR* likely encodes a pathway-specific activator of the PZN  
94 biosynthetic gene cluster. To interrogate whether *pyrR* could activate this biosynthetic pathway, we  
95 introduced an additional copy of *pyrR* into *S. candidus* NRRL 3601 under the control of a  
96 constitutive promoter to release the transcriptional control from higher-level regulatory mechanisms.  
97 Subsequent metabolic profiling of the resulting strain *S. candidus* *pyrR*-OE by LC-MS together with  
98 NMR analysis of isolated PZN demonstrated that PZN production was successfully recovered, with  
99 a PZN yield of ~10 mg/L (**Fig. 2b and 2c, Fig. S1**). Furthermore, RT-PCR analysis of selected *pyr*  
100 genes revealed their active transcription in *S. candidus* *pyrR*-OE, including the *spb40* homolog *pyrN*,  
101 which is located in a putative operon consisting of genes *pyrKLMN* (**Fig. 2d**). Altogether, these  
102 results demonstrated that PyrR is a transcriptional activator governing PZN biosynthesis, and by  
103 extension, the *pyr* cluster is responsible for PZN biosynthesis.

104 We next interrogated the biosynthetic origin of N-1 and N-2 in the pyrazole ring of PZN, which  
105 remain obscure despite the previous isotope feeding experiments and our *in silico* analysis of the  
106 *pyr* cluster. The presence of *spb38* and *spb40* homologs *pyrM* and *pyrN* in the *pyr* cluster indicate  
107 that a N-N bond forming mechanism analogous to that of the s56-p1 pathway might operate in PZN  
108 biosynthesis.<sup>[7]</sup> We envisaged two possible routes that could afford the hydrazine moiety in the  
109 pyrazole ring (**Fig. 3a**). In one scenario, the Spb40 homolog PyrN could catalyze N-N bond  
110 formation between the N-6 nitrogen of L-*N*<sup>6</sup>-OH-Lys with another amine-containing substrate to  
111 generate a molecule as a hydrazine carrier, which would be followed by the transfer of the hydrazine  
112 moiety to a glutamate or  $\alpha$ -KG derivative by downstream pathway enzymes. In this scenario, PyrN  
113 could be functionally equivalent to Spb40 and produce the product Lys-Gly for the subsequent  
114 hydrazine transfer. A second scenario involves the direct installation of hydrazine moiety on  
115 glutamate or its derivative, through linking the  $\alpha$ -NH<sub>2</sub> of glutamate (or its derivative) to N-6 nitrogen  
116 of L-*N*<sup>6</sup>-OH-Lys. The resulting product could then be processed by other *pyr* enzymes to furnish the  
117 pyrazole ring. To distinguish between these two possible routes, we first separately fed L-<sup>15</sup>N-Gly  
118 or L-<sup>15</sup>N-Glu (at concentrations of 3 mM) into the culture of *S. candidus* *pyrR*-OE and analyzed the  
119 isotope incorporation of PZN by LC-MS. We found that the nitrogen from the  $\alpha$ -NH<sub>2</sub> of glutamate

120 efficiently incorporated into PZN, with the relative intensity of +1 Da peak increasing from 11% to  
121 46% when compared to unlabeled PZN (**Fig. S2**). Furthermore, the +2 Da peak increased to 16 %.  
122 By contrast, only minor incorporation of the nitrogen from <sup>15</sup>N-Gly was detected. Although it is  
123 likely that the observed incorporation pattern is due to or partially attributed to scrambling of the  
124 labels by primary metabolism, this result favors the second scenario, where the N-1, and by  
125 extension, C-3 to C-6 atoms, in the pyrazole moiety might derive from L-Glu as an intact unit (**Fig.**  
126 **3a**).

127 To gain further insights into the product from the PyrN-catalyzed reaction, we adopted an *in*  
128 *vivo* reconstitution method by introducing *pyrN* into the *E. coli* strain expressing *nbtG*. NbtG, a  
129 homolog of PyrM and Spb38, is a well-characterized lysine <sup>N</sup>6-hydroxylase and thus could provide  
130 endogenous L-OH-<sup>N</sup>6-Lys *in vivo*. LC-MS analysis of culture supernatant from the *E. coli* strain  
131 carrying both *nbtG* and *pyrN* revealed the presence of a molecule with a MS signal at *m/z* 292, which  
132 is absent from that of *E. coli* strain expressing either *nbtG* or *pyrN* (**Fig. 3b**). This MS signal (*m/z*  
133 292) is consistent with the [M+H]<sup>+</sup> ion of a Lys-Glu conjugate product (**1**) (**Fig. 3a**). No MS signal  
134 (*m/z* 220) of Lys-Gly was detected, supporting that Gly is not a substrate of PyrN, in contrast to  
135 Spb40. To track the origin of compound **1**, we fed the strain *E. coli/nbtG+pyrN* with different  
136 combinations of <sup>13</sup>C/<sup>15</sup>N-labeled and unlabeled amino acid precursors, including L-<sup>13</sup>C<sub>6</sub>-Lys, L-<sup>15</sup>N-  
137 Glu, L-<sup>15</sup>N-Gly (**Fig. S3**). Compared with cultures supplemented with unlabeled amino acids, the  
138 compound **1** produced in the presence of L-<sup>13</sup>C<sub>6</sub>-Lys showed the appearance of a strong +6 Da MS  
139 signal (*m/z* 298.1), supporting the incorporation of an intact lysine carbon skeleton. While **1**  
140 produced with the addition of <sup>15</sup>N-Gly showed a similar isotope pattern to the one fed with unlabeled  
141 amino acids, addition of <sup>15</sup>N-Glu resulted in significant enrichment of +1 Da signal, with an increase  
142 in the relative intensity from 12 % to 45 %. Fmoc-chloride treatment of the *E. coli* culture  
143 supernatants supplemented with <sup>13</sup>C<sub>6</sub>-Lys, followed by LC-HR-MS analysis, resulted in the  
144 detection of a strain-specific metabolite from *E. coli/nbtG+pyrN* with MS signals at *m/z* 514.2164  
145 and 520.2364, which are consistent with the [M+H]<sup>+</sup> ion of Fmoc-Lys-Glu and Fmoc-(<sup>13</sup>C<sub>6</sub>)Lys-Glu  
146 conjugate, respectively (**Fig. 4a** and **Fig. S4**). Our attempt to isolate this molecule for NMR analysis  
147 was hampered by its low yield and instability. However, the fragmentation pattern of **1** from LC-  
148 HR-MS/MS analysis after Fmoc-Cl derivatization, together with the sequence homology between  
149 PyrN and Spd40, supports that **1** most likely arises from linking the  $\alpha$ -NH<sub>2</sub> of glutamate with the  $\epsilon$ -

150 NH<sub>2</sub> of lysine (**Fig. 4b and 4c**).<sup>[7]</sup> Altogether, the above results suggested that PyrM and PyrN  
151 together mediate the conjugation L-Glu and L-Lys though a N-N linkage.

152 As in Spb40, the residues potentially involved in ATP-binding and metal-chelating are also  
153 conserved in the aaRS-like and cupin domains of PyrN, respectively (**Fig. S5 and S6**). Consistent  
154 with this *in silico* analysis, inductively coupled plasma mass spectrometry (ICP-MS) analysis of the  
155 purified His-tagged PyrN demonstrated that it contains two equivalents of zinc, supporting the  
156 presence of a single, conserved zinc coordination site in each domain (**Fig. S7**). Even though we  
157 were able to obtain soluble recombinant PyrN, our preliminary screening of reaction conditions for  
158 the *in vitro* assay of PyrN did not produce any detectable product so far, which could be attributed  
159 to yet-unknown factors necessary for this reaction. Nonetheless, we expect that the PyrN reaction  
160 mechanism is likely to be similar to that has been suggested for Spb40, where there is a similar lack  
161 of *in vitro* work reported in the literature.<sup>[7]</sup> Based on the results from our *in vivo* reconstitution in  
162 *E. coli* and previous isotope tracking experiments on Spb40 (**Fig. S8**), the C-terminal aaRS-like  
163 domain of PyrN is likely responsible for glutamate carboxylate activation, to afford glutamyl-  
164 adenylate or further to give glutamyl-tRNA, which could then undergo ligation to the hydroxyl  
165 group of L-OH-*N*<sup>6</sup>-Lys to form an ester intermediate, and followed by rearrangement to generate **1**,  
166 which is likely mediated by the N-terminal cupin domain. Formation of an ester intermediate by the  
167 conjugation of an amino acid to a hydroxylamine, using aminoacyl-tRNA as a carrier, is not  
168 unprecedented. In the biosynthesis of azoxy-containing valanimycin, the seryl-tRNA synthetase  
169 VlmL produces L-seryl-tRNA, followed by VlmA-mediated seryl transfer to isobutylhydroxylamine  
170 to form *O*-seryl-isobutylhydroxylamine, which then undergoes subsequent transformation(s) for N-  
171 N bond formation.<sup>[19]</sup> Following the formation of **1**, the next step in the PZN pathway is likely  
172 catalyzed by PyrL, whose encoding gene *pyrL* appears to be located in the same operon with *pyrM*  
173 and *pyrN*, indicating their functional relevance (**Fig. 2a**). PyrL displays sequence homology to  
174 saccharopine dehydrogenase. In lysine metabolism, saccharopine dehydrogenase mediates  
175 reversible conversion of saccharopine to L-2-amino adipate-6-semialdehyde (AASA) and L-Glu (**Fig.**  
176 **S9**).<sup>[25]</sup> PyrL might thus catalyze an analogous reaction, converting **1** to AASA and 2-  
177 hydrazinogluutaric acid (**2**), the latter of which could then be processed by downstream pathway  
178 enzymes for pyrazole ring assembly (**Fig. 4d**).

179 In conclusion, we have identified the gene cluster responsible for pyrazomycin biosynthesis in

180 *S. candidus* NRRL 3601, and demonstrated that PyrR is a new member of the StrR family  
181 transcriptional activator controlling PZN biosynthesis. Furthermore, our current data strongly  
182 supports that PyrN is a new N-N bond forming enzyme, and the formation of the lysine-glutamate  
183 conjugate through a N-N linkage could be the starting point for the PZN biosynthetic pathway. This  
184 study paves the way for further biochemical characterization of PyrN and other PZN pathway  
185 enzymes involved in the assembly of the unique pyrazole ring.

186

187 **Experimental Section**

188 Full experimental details are available in the Supporting Information

189

190 **Acknowledgements**

191 This work was supported by funding from National Key R&D Program of China  
192 (2018YFA0903203), the National Natural Science Foundation of China (31872625), the Zhejiang  
193 Provincial Science Foundation (LR19C010001) and the Natural Sciences and Engineering Research  
194 Council of Canada (RGPIN-2016-03778).

195

196 **Keywords:** biosynthesis • N-N bond • pyrazole • C-nucleoside • pathway activator

197

198 **References**

- 199 [1] L. M. Blair, J. Sperry, *J. Nat. Prod.* **2013**, *76*, 794–812.
- 200 [2] Y.-L. Du, H.-Y. He, M. A. Higgins, K. S. Ryan, *Nature Chemical Biology* **2017**, *13*, 836–838.
- 201 [3] T. L. Ng, R. Rohac, A. J. Mitchell, A. K. Boal, E. P. Balskus, *Nature* **2019**, *566*, 94.
- 202 [4] H.-Y. He, A. C. Henderson, Y.-L. Du, K. S. Ryan, *J. Am. Chem. Soc.* **2019**, *141*, 4026–4033.
- 203 [5] Y. Sugai, Y. Katsuyama, Y. Ohnishi, *Nature Chemical Biology* **2016**, *12*, 73–75.
- 204 [6] A. J. Waldman, E. P. Balskus, *J. Org. Chem.* **2018**, *83*, 7539–7546.
- 205 [7] K. Matsuda, T. Tomita, K. Shin-ya, T. Wakimoto, T. Kuzuyama, M. Nishiyama, *J. Am. Chem. Soc.* **2018**, *140*,  
206 9083–9086.
- 207 [8] K.-K. A. Wang, T. L. Ng, P. Wang, Z. Huang, E. P. Balskus, W. A. van der Donk, *Nature Communications*  
208 **2018**, *9*, 3687.
- 209 [9] R. P. Garg, X. L. Qian, L. B. Alemany, S. Moran, R. J. Parry, *PNAS* **2008**, *105*, 6543–6547.

210 [10] Z. Huang, K.-K. A. Wang, W. A. van der Donk, *Chem. Sci.* **2016**, *7*, 5219–5223.

211 [11] J. M. Winter, A. L. Jansma, T. M. Handel, B. S. Moore, *Angewandte Chemie International Edition* **2009**, *48*,  
212 767–770.

213 [12] Q. Zhang, H. Li, L. Yu, Y. Sun, Y. Zhu, H. Zhu, L. Zhang, S.-M. Li, Y. Shen, C. Tian, et al., *Chem. Sci.* **2017**,  
214 *8*, 5067–5077.

215 [13] M. Baunach, L. Ding, T. Bruhn, G. Bringmann, C. Hertweck, *Angewandte Chemie International Edition* **2013**,  
216 *52*, 9040–9043.

217 [14] F. F. Twigg, W. Cai, W. Huang, J. Liu, M. Sato, T. J. Perez, J. Geng, M. J. Dror, I. Montanez, T. L. Tong, et  
218 al., *ChemBioChem* **2019**, *20*, 1145–1149.

219 [15] R. Williams, M. Hoehn, *Pyrazomycin and Process for Production Thereof*, **1974**, US3802999A.

220 [16] K. Gerzon, D. C. Delong, J. C. Cline, *Pure and Applied Chemistry. Chimie Pure et Appliquee*; Berlin **1971**, *28*,  
221 489–498.

222 [17] G. Xu, L. Kong, R. Gong, L. Xu, Y. Gao, M. Jiang, Y.-S. Cai, K. Hong, Y. Hu, P. Liu, et al., *Appl. Environ.*  
223 *Microbiol.* **2018**, *84*, e01860-18.

224 [18] P. Wu, D. Wan, G. Xu, G. Wang, H. Ma, T. Wang, Y. Gao, J. Qi, X. Chen, J. Zhu, et al., *Cell Chemical Biology*  
225 **2017**, *24*, 171–181.

226 [19] S.-A. Wang, Y. Ko, J. Zeng, Y. Geng, D. Ren, Y. Ogasawara, S. Irani, Y. Zhang, H. Liu, *J. Am. Chem. Soc.*  
227 **2019**, *141*, 6127–6131.

228 [20] J. W. Scott, M. E. Rasche, *Journal of Bacteriology* **2002**, *184*, 4442–4448.

229 [21] L. Retzlaff, J. Distler, *Molecular Microbiology* **1995**, *18*, 151–162.

230 [22] A. Tomono, Y. Tsai, H. Yamazaki, Y. Ohnishi, S. Horinouchi, *Journal of Bacteriology* **2005**, *187*, 5595–5604.

231 [23] A. S. Eustáquio, S.-M. Li, L. Heide, *Microbiology* **2005**, *151*, 1949–1961.

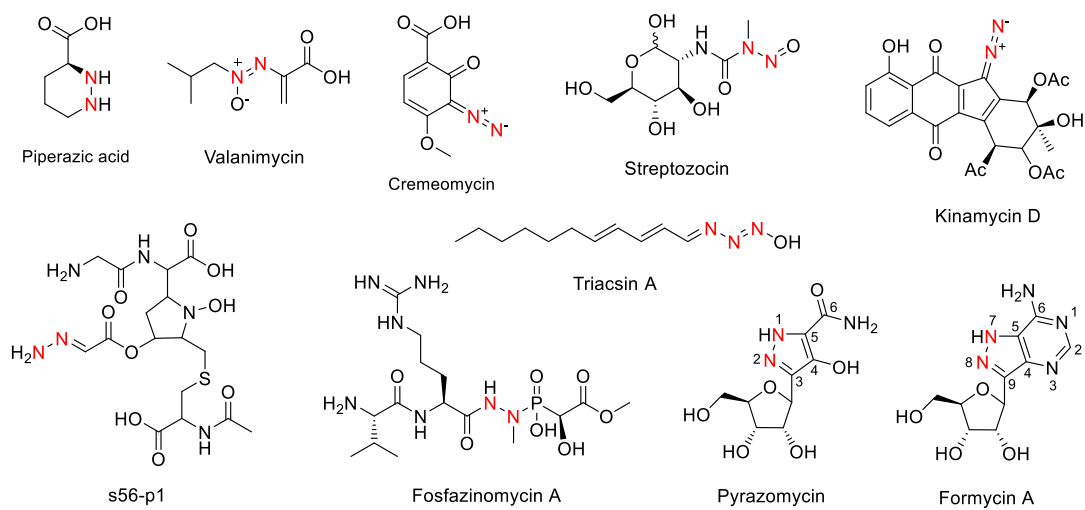
232 [24] R. M. Shawky, O. Puk, A. Wietzorre, S. Pelzer, E. Takano, W. Wohlleben, E. Stegmann, *MMB* **2007**, *13*, 76–  
233 88.

234 [25] D. R. Storts, J. K. Bhattacharjee, *Journal of Bacteriology* **1987**, *169*, 416–418.

235

236 **Figure 1.** Examples of natural products containing a nitrogen-nitrogen linkage.

237

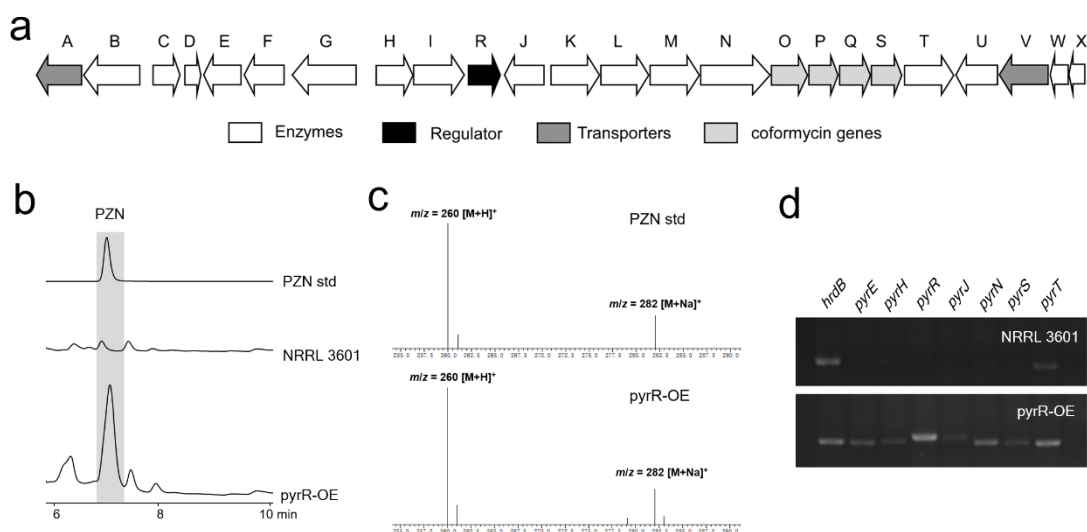


238

239

240 **Figure 2.** Identification of the gene cluster and cluster-situated activator for pyrazomycin  
241 biosynthesis. **(a)** The biosynthetic gene cluster of pyrazomycin. **(b)** HPLC analysis of the culture  
242 supernatants from strain *S. candidus* NRRL 3601 and its *pyrR*-overexpression mutant *pyrR*-OE. **(c)**  
243 MS analysis of the pyrazomycin standard compound and the new product produced by strain *pyrR*-  
244 OE. **(d)** Transcriptional analysis of selected genes from *pyr* gene cluster in strain NRRL 3601 and  
245 *pyr*-OE by RT-PCR.

246



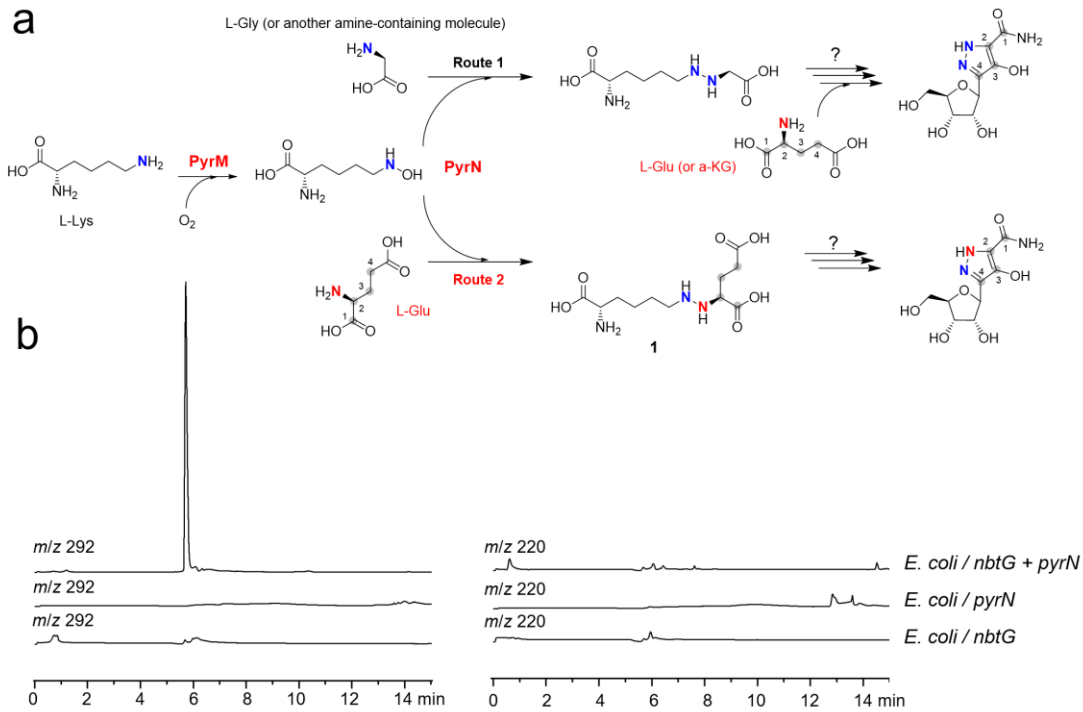
247

248

249

250

251 **Figure 3. (a)** Possible biosynthetic routes to the pyrazole ring in pyrazomycin based on previous  
252 studies. **(b)** LC-MS analysis of engineered *E. coli* strains carrying different gene(s).

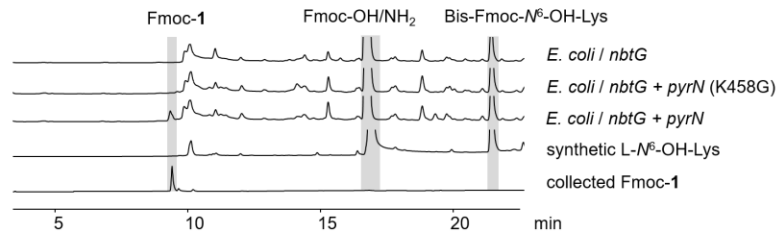


253

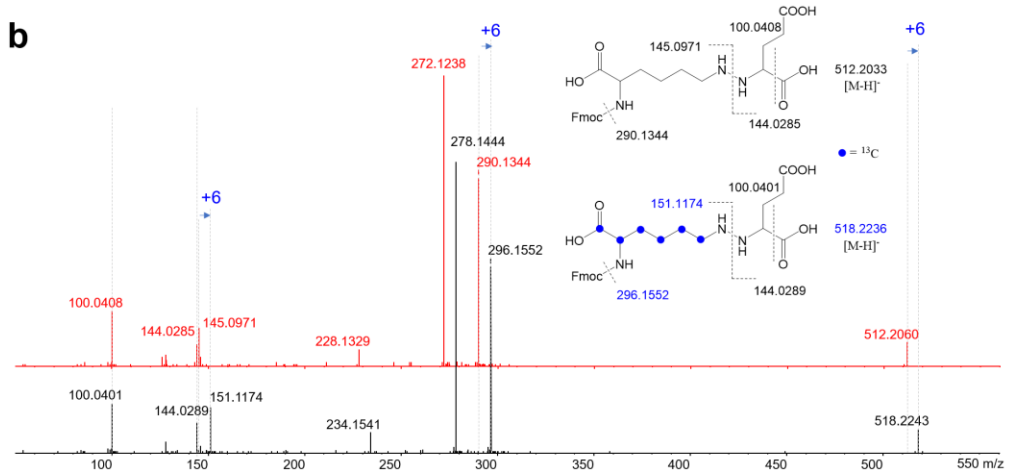
254

255 **Figure 4.** The *in vivo* reconstitution of the PyrN-catalyzed reaction in *E. coli* and proposed  
256 biosynthetic origin of the pyrazole ring in pyrazomycin. **(a)** HPLC analysis of culture supernatants  
257 from the *E. coli* strains containing different gene combinations after Fmoc-Cl derivatization. Note:  
258 Lys458 is a residue potentially involved in ATP-binding in PyrN (see below in the main text). **(b)**  
259 and **(c)** LC-HR-MS/MS analysis of the strain-specific metabolites from *E. coli* / *nbtG* + *pyrN*  
260 supplemented with L-<sup>13</sup>C<sub>6</sub>-Lys under negative and positive modes, respectively. Note: the red  
261 traces are from the MS/MS analysis of unlabeled molecules, and the black traces are from <sup>13</sup>C<sub>6</sub>-  
262 labeled molecules. **(d)** Proposed biosynthetic origin of the pyrazole moiety in pyrazomycin based  
263 on the results from this study and previous stable-isotope precursor feeding experiments.

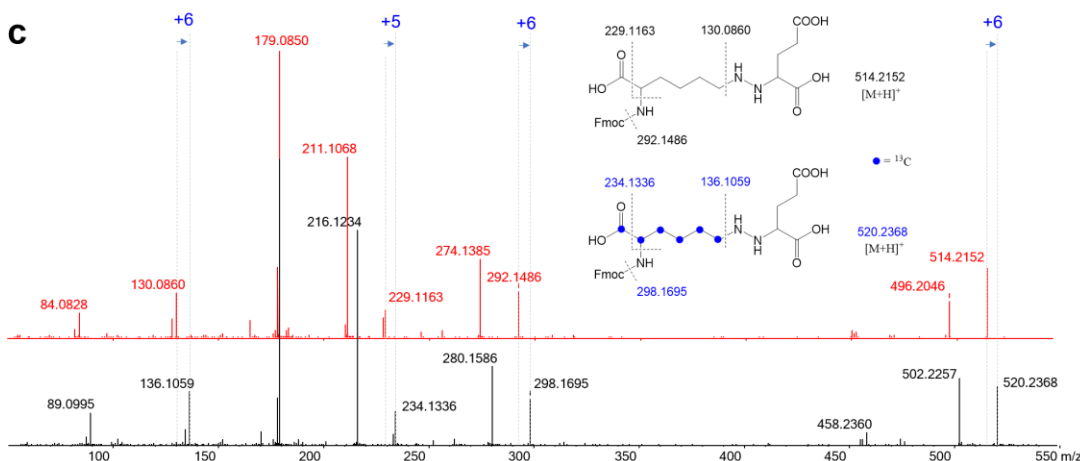
**a**



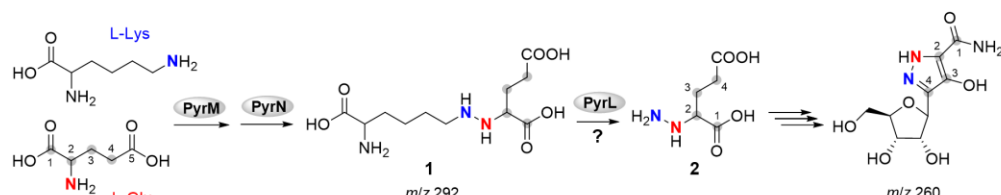
**b**



**c**



**d**



264

265